Nuclear Physics B42 (1972) 1–28. North-Holland Publishing Company

8.A.3

ANTIPROTON PROTON ANNIHILATIONS AT 1.6–2.2 GeV/c INTO FINAL STATES WITH A K_1^0 MESON*

J.W. CHAPMAN, T.M. CHURCH**, J. LYS, C.T. MURPHY***, H.M. RING‡, and J.C. VANDER VELDE
The University of Michigan, Ann Arbor, Michigan 48104

Received 4 January 1972

Abstract: Antiproton proton annihilations into final states containing at least one K_1^0 meson have been studied in a 150 000 picture bubble chamber experiment. The experiment covered six incident antiproton momenta in the range 1.6–2.2 GeV/c. Cross sections at each incident momentum are determined for the more abundantly produced final states, and momentum averaged cross sections are determined for some rarer final states, including $K^0\overline{K}^0$ and $K^0\overline{K}^0K^+K^-$. Copious resonance production, including double resonance production, is observed, and percentage contributions of different resonance channels are evaluated. Cross sections and resonance fractions are compared with results of other experiments at antiproton momenta in the range 0.7–3.7 GeV/c.

1. INTRODUCTION

Antiproton-proton annihilations into final states containing at least one visible K_1^0 decay have been studied at six incident antiproton momentum in the range 1.6–2.2 GeV/c in a bubble chamber experiment. The six momenta (total c.m. energy) were 1.62 GeV/c (2294 MeV), 1.76 (2347), 1.82 (2368), 1.88 (2389), 1.94 (2410), and 2.20 (2500). The sensitivity at each momentum was ~ 0.6 events per μb of cross section.

Cross sections for all final states were determined at each momentum. Copious production of K*, ρ and ω mesons was observed, and there was also evidence for A_2, D, and ϕ production. The percentage contributions of resonance channels to the various final states were evaluated, assuming that different processes are incoherent and using Lorentz-invariant phace space. No evidence for violation of charge conjugation

* Work supported by the U.S. Atomic Energy Commision.
** Present Address: Laboratory for Nuclear Science, Massachusetts Institute of Technology, Cambridge, Ma.
*** Present address: Carnegie-Mellon University, Pittsburgh, Pa.
‡ Present address: The Cyphernetics Corporation, 175 Jackson Plaza, Ann Arbor, Mi.

symmetry (or *CP* invariance) was observed, so normally charge conjugate reactions were combined. Our results are compared with results of other experiments at various incident antiproton momenta.

The final states $K_1^0K_1^0\pi^+\pi^-\pi^0$, $K_1^0K^\pm\pi^\mp\pi^+\pi^-$, and $K_1^0\pi^+\pi^-K_2^0m\pi^0$ ($m \geq 1$) observed in this experiment have been reported previously, together with the $K^+K^-\pi^+\pi^-\pi^0$ final state, in a paper dealing with $\bar{p}p \to \bar{K}K\pi\pi\pi$, where the main emphasis was on possible direct channel resonances. Reference to other $\bar{p}p$ reactions studied with the same bubble chamber film may be found in that paper. More detailed accounts of V–production may be found in refs. [2, 3].

2. SCANNING AND MEASURING

The entire film (150 000 pictures) was double scanned for V events. The events found were disagreement scanned, measured, and processed through the pregeometry, geometry, and kinematics programs CAST, TVGP, and SQUAW. Three remeasurement passes were made.

A V was accepted as a good K_1^0 if its 3–constraint fit to a K_1^0 decay from an acceptable beam track interaction ("ponting" fit) had a confidence level $> 10^{-6}$. If the V also fit as Λ or $\bar{\Lambda}$ decay, then if only one of the fits had confidence level $> 10^{-2}$ that fit was accepted. otherwise the ambiguity was resolved by examining bubble densities. Since the energies of this experiment are above the $\Lambda\bar{\Lambda}$ threshold but below the $\Lambda\bar{\Lambda}\pi^+\pi^-$ threshold, this ambiguity only occurred with zero-prong beam interactions.

Events that failed to pass the reconstruction programs after the remeasurements were examined at the scan table. From those that appeared to be good events (usually with some special measurement difficulty), an appropriate correction factor was determined, which varied from ~ 9% for 4–prong events to 1.6% for 0–prong events. There was a very small incident momentum dependence.

Vees that fit the 1–constraint hypothesis $K_1^0 \to \pi^+\pi^-$, but failed the 3–constraint "pointing" fit on all measurements, and were not Λ or $\bar{\Lambda}$, were reexamined at the scan table for possible overlooked origins. The number found to have previously undiscovered acceptable origins was less than 0.5% of the number of accepted K_1^0. Thus we believe that there is no unaccounted for loss of events resulting from mismeasurement, misidentification of origin, or inadequacies of the fitting program.

Table 1
Numbers of accepted K_1^0 events in the fiducial volume.

Main vertex prongs	1–V	2–V
0	274	86
2	2379	442
4	637	12
6	0	0

For V events with prongs, the scanning efficiency was calculated from the double scan to be 0.98 for 1–V events and 0.99 for 2–V events. The results of a triple scan of some of the film was used to calculate the scan efficiencies for 0–prong events, and gave 0.90 (±0.04) for 1–V events and 0.99 for 2–V events. The lower efficiency for 0–prong 1–V events is not unreasonable.

The final (uncorrected) numbers of accepted K_1^o events, after a fiducial volume cut, are given by event topology in table 1. There was also one 0–prong 3–V event.

3. RESOLUTION OF FINAL STATES

The kinematic fitting program performed a multivertex fit to each of the various possible hypotheses, if one or more Vs satisfied the pointing fit. A main vertex χ^2 was defined for each fit as the difference between the χ^2 values of the multivertex fit and the pointing V fit (or fits if a 2–V event. The confidence level derived from this main vertex χ^2, using the appropriate number of constraints (usually 4 or 1) was used to select the acceptable fits amongst those attempted.

Of the 0–prong 2–V events, only one fit the hypothesis $K_1^oK_1^o$ with a main vertex confidence level $> 10^{-6}$ (the one had a confidence level of 50%). The 24 events that fit the $K_1^oK_1^o\pi^o$ hypothesis with confidence level $> 10^{-2}$ were accepted as $K_1^oK_1^o\pi^o$ events, while the remaining 61 events were assigned to $K_1^oK_1^om\pi^o$, $m \geq 2$. A missing mass plot (fig. 1(a)) showed essentially no overlap between these two categories.

Of the 0–prong 1–V events, 10 had a missing mass in the range 300–600 MeV, and were accepted as $K_1^o(K^o)$ events, while the other 70 were assigned to the class $K_1^oK^om\pi^o$, $m \geq 1$. The missing mass plot (fig. 1(b)) showed that there was no overlap between these two categories.

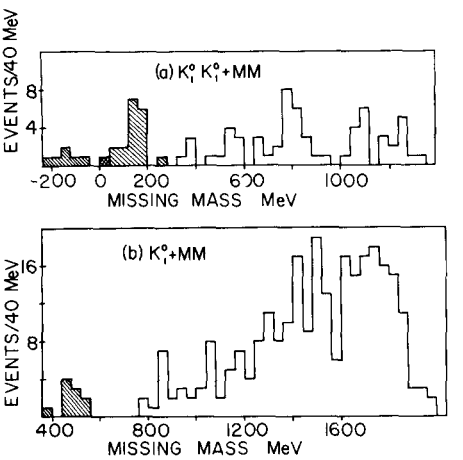

Fig. 1. Calculated missing mass for 0–prong events. (a) 2–V events: shaded events are $K_1^oK_1^o\pi^o$, cross-hatched event is $K_1^oK_1^o$. (b) 1–V events: shaded events are $K_1^o(K^o)$.

The 2–prong 2–V events that fit with confidence level $> 10^{-6}$ either the 4–constraint $K_1^oK_1^o\pi^+\pi^-$ hypothesis or the 1–constraint $K_1^oK_1^o\pi^+\pi^-\pi^o$ hypothesis were accepted as that event type. Six events fit both, but all favored the former hypothesis and were taken to be $K_1^oK_1^o\pi^+\pi^-$ events. The remaining events of this topology were assigned to $K_1^oK_1^o\pi^+\pi^- m\pi^o$, $m \geq 2$. From a missing mass plot it was estimated that the number of events of this last type that were erroneously taken as $K_1^oK_1^o\pi^+\pi^-\pi^o$ events was $\lesssim 1\%$ of the $K_1^oK_1^o\pi^+\pi^-\pi^o$ events.

In the 2–prong 1–V and 4–prong 1–V events, there were numerous kinematic ambiguities between various final state hypotheses. Therefore all these events were examined in a special bubble density scan. The scanners were given, for each prong of an event, the projected ionizations for both kaon and pion hypotheses, using unfitted momenta, as well as beam and V ionizations. Normally a decision on a track could be made if the momentum was less than ~ 700 MeV/c, corresponding to a relative K to π ionization ratio of 1.44 (in a bubble chamber with good clear tracks, we tended to be a little conservative here). The bubble density information was combined with the kinematic fit results to determine the correct final state for each event. A kinematic fit was deemed acceptable if the confidence level was greater than 10^{-3} for 4–constraint fits (i.e. no missing neutral particle) or 10^{-2} for 1–constraint fits (one missing neutral particle). A missing mass "fit" (two or more missing neutral particles) was acceptable if the calculated missing mass plus twice its error was greater than the minimum possible (i.e. $2m(\pi^o)$ or $m(K^o) + m(\pi^o)$, m = mass).

The requirement that an acceptable constrained or missing mass fit be compatible with the bubble density information, and a preference for constrained over missing mass fits if both were acceptable and compatible with bubble density, served to give a unique final state to most events. However, some events did remain ambiguous,

Table 2
Ambiguous 2–prong events.

Final states	Number of events
$K_1^oK^+\pi^-$, $K_1^oK^-\pi^+$	7
$K_1^oK^+\pi^-\pi^o$, $K_1^oK^-\pi^+\pi^o$	14
$K_1^oK^+\pi^-\pi^o$, $K_1^o\pi^+\pi^-(K^o)$	39
$K_1^oK^-\pi^+\pi^o$, $K_1^o\pi^+\pi^-(K^o)$	35
$K_1^oK^+\pi^-\pi^o$, $K_1^oK^-\pi^+\pi^o$, $K_1^o\pi^+\pi^-(K^o)$	9
$K_1^o\pi^+\pi^-M$, $K_1^oK^+\pi^-M$	54
$K_1^o\pi^+\pi^-M$, $K_1^oK^-\pi^+M$	56
$K_1^o\pi^+\pi^-M$, $K_1^oK^+\pi^-M$, $K_1^oK^-\pi^+M$	10
$K_1^oK^+K^-(K^o)$, $K_1^oK^+\pi^-M$ or $K_1^oK^-\pi^+M$	7

M indicates more than one missing neutral particle. (K^o) indicates an unseen $K^o - K_1^o$ or K_2^o.

viz. 231 out of 2379 2–prong events and 4 out of 637 4–prong events. The small number of 4–prong ambiguities results from the small number of missing mass events with 4 prongs and the lower laboratory momentum of the particles. The fraction of charged kaons with momenta less than 700 MeV/c was 0.31, 0.55, 0.76, and 0.83 respectively for 3, 4, 5, and 6–body annihilations. Details of the 2–prong ambiguous events are given in table 2. In the calculation of cross sections, the ambiguous events were assumed to divide up into the competing final states in the same ratios as the unambiguous events.

Plots of the missing mass and the kinematic fit χ^2, with and without cuts on the momenta of the charged tracks, showed that the events which were assigned to 4–constraint fit final states were in fact very clean, with an estimated contamination of $< 2\%$. Some contamination of the 1–constraint fit final states is possible from missing mass events; such contamination was estimated to be $< 5\%$ for the 2–prongs and $< 3\%$ for the 4–prongs.

A very few events, 22 two–prongs and 18 four–prongs, had no acceptable fit compatible with bubble density, and were classified as "rejected". Most of these were considered to arise from the confidence level cut-offs mentioned above. Confidence

Table 3
Final states of unambiguous 1–V events.

Final state	Number
$K_1^0(K^0)$	10
K_1^0M	264
$K_1^0K^+\pi^-$ + cc.	221
$K_1^0K^+\pi^-\pi^0$ + cc.	599
$K_1^0\pi^+\pi^-(K^0)$	440
$K_1^0K^+\pi^-M$ + cc.	332
$K_1^0\pi^+\pi^-M$	524
$K_1^0K^+K^-(K^0)$	10
$K_1^0K^+\pi^+\pi^-\pi^-$ + cc.	347
$K_1^0K^+\pi^+\pi^-\pi^-\pi^0$ + cc.	192
$K_1^0\pi^+\pi^+\pi^-\pi^-(K^0)$	24
$K_1^0K^+\pi^+\pi^-\pi^-M$ + cc. $K_1^0\pi^+\pi^+\pi^-\pi^-M$	50
$K_1^0K^+K^+K^-\pi^-$ + cc.	2

M indicates more than one missing neutral particle.
(K^0) indicates an unseen $K^0 - K_1^0$ or K_1^0.
cc. stands for charge conjugate.

Table 4
Final states of unambiguous 2–V events

Final state	Number
$K_1^0K_1^0$	1
$K_1^0K_1^0\pi^0$	24
$K_1^0K_1^0$M	61
$K_1^0K_1^0\pi^+\pi^-$	177
$K_1^0K_1^0\pi^+\pi^-\pi^0$	207
$K_1^0K_1^0\pi^+\pi^-$M	43
$K_1^0K_1^0K^+K^-$	1
$K_1^0K_1^0\pi^+\pi^+\pi^-\pi^-$	12
$K_1^0K_1^0\pi^+\pi^+\pi^-\pi^-\pi^0$	2

M indicates more than one missing neutral particle.

level plots for accepted fits were generally fairly flat, with a small tail at < 0.01 for the 4–constraint fits. Hence this number of rejects is not unreasonable.

The final numbers of events unambiguously assigned to the different final states are listed in tables 3 and 4 respectively for 1–V and 2–V topologies.

4. CROSS SECTIONS

A count of the number of good beam tracks on every twentieth frame, and a computation of the average path length of a beam track in the fiducial volume, enabled event numbers to be converted into microbarns of cross section. The resulting microbarns per event at the six beam momenta were 1.85 (1.62 GeV/c), 1.64 (1.76), 1.61 (1.82), 1.37 (1.88), 1.58 (1.94), and 1.54 (2.20). A study of delta rays on a sample of pictures showed that the contamination of the beam by pions and muons was 0.4%.

Before converting events into microbarns, each event was weighted according to the probability that the K_1^0(s) decay in our fiducial volume. The fiducial volume for a beam track interaction was made smaller than that for V decays to avoid large weights. In addition, for all except the 2 and 4–prong 2–V events, a close cut was imposed and a corresponding weight calculated. For 2 and 4–prong 1–V events, the close cut was a 4 mm radius sphere centred at the beam interaction point, and for the 0–prong events an ellipsoid (5 mm by 5 mm by 2.5 mm) was used. The resulting weight for an event (both sources combined) averaged $\sim$ 1.20, and was very seldom greater than 1.50.

Various corrections were applied to the raw cross sections calculated from the

weighted events. These corrections were for the scanning ineffeciency and remeasurement failures mentioned earlier, for $K_1^o \to \pi^o\pi^o$ decays using a $K_1^o \to \pi^+\pi^-$ branching ratio of 0.684, and for very small or very large angle K_1^o decays. The last correction was applied because such Vs are not so easy to recognise in scanning (scan efficiency calculations omitted these extremes), and was determined from plots of the K_1^o c.m. decay angle to be 0.97 for 1–V events, 1.00 for 2–V events.

The final cross sections at each beam momentum are given in table 5 for various final states. Cross sections averaged over the four central beam momenta are given in table 6 for some final states with small numbers of events. The errors take into

Table 5
Final state cross sections (in microbarns)

	Beam Momentum (GeV/c)					
	1.62	1.76	1.82	1.88	1.94	2.20
$K_1^oK^+\pi^-$ + cc.	203	104	100	103	102	78
error	28	19	18	17	18	15
$K_1^oK^+\pi^-\pi^o$ + cc.	386	304	274	353	323	278
error	40	33	31	33	33	30
$K_1^oK_1^o\pi^+\pi^-$	107	139	136	138	132	107
error	25	28	27	26	26	23
$K_1^oK_2^o\pi^+\pi^-$	251	150	201	152	107	125
error	36	34	35	31	28	28
$K_1^oK^+\pi^+\pi^-\pi^-$ + cc.	181	212	183	181	179	161
error	27	28	25	24	25	24
$K_1^oK_1^o\pi^+\pi^-\pi^o$	117	172	200	136	106	151
error	27	31	34	26	23	29
$K_1^oK^+\pi^+\pi^-\pi^-\pi^o$ + cc.	67	79	99	123	104	136
error	17	17	18	19	19	22
$K_1^o(K_2^o m\pi^o, m \geq 1)$	108	58	141	126	99	85
error	29	27	30	24	23	24
$K_1^oK_1^oM$	54	94	35	36	28	53
error	17	24	13	12	11	15
$K_1^oK^+\pi^-M$ + cc.	204	169	176	167	185	201
error	28	24	24	22	24	25
$K_1^o\pi^+\pi^-(K_2^o m\pi^o, m \geq 1)$	237	176	168	229	192	156
error	39	39	39	34	33	36

M indicates more than one missing neutral particle.

Table 6
Final state cross sections (σ) averaged over antiproton momenta 1.76–1.94 GeV/c (in microbarns).

Final state	σ	error
$K_1^0K_1^0$	1	1
$K_1^0K_2^0$	5	2
$K_1^0K_1^0\pi^0$	18	5
$K_1^0K_1^0\pi^+\pi^-$M	36	6
$K_1^0K_1^0\pi^+\pi^+\pi^-\pi^-$	5	2
$K_1^0K_2^0\pi^+\pi^+\pi^-\pi^-$	9	4
$K_1^0K_2^0K^+K^-$	8	3

M indicates more than one missing neutral particle

account errors in the events to microbarns conversion factor, in the corrections applied, and in the ambiguous events assignments, as well as the statistical errors in the numbers of events. In all cases the last of these dominates.

The cross sections for final states containing a K_2^0 were derived from the numbers of the appropriate $K_1^0K_1^0$ (+ pions) and $K_1^0(K^0)$ (+ pions) events, where (K^0) denotes

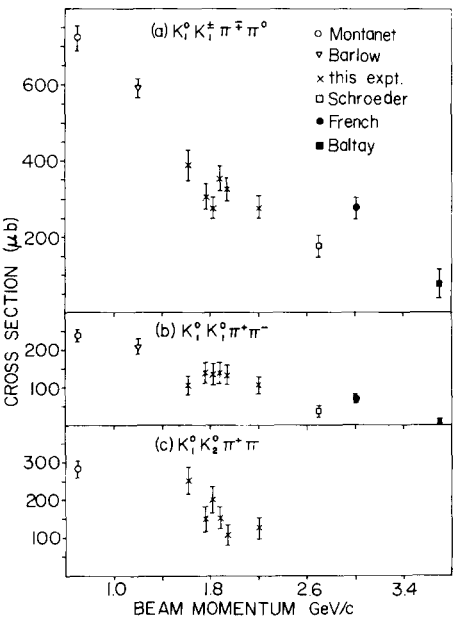

Fig. 2. Cross sections for (a) $\bar{p}p \to K_1^0K^\pm\pi^\mp\pi^0$; (b) $\bar{p}p \to K_1^0K_1^0\pi^+\pi^-$; (c) $\bar{p}p \to K_1^0K_2^0\pi^+\pi^-$.

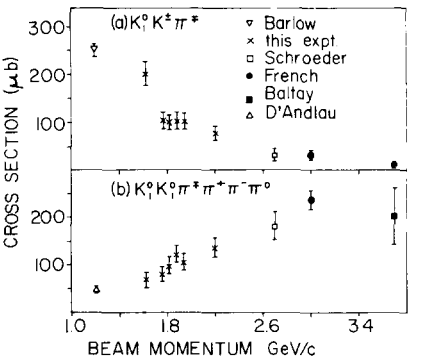

Fig. 3. Cross sections for (a) $\bar{p}p \to K^0_1 K^\pm \pi^\mp$; (b) $\bar{p}p \to K^0_1 K^\pm \pi^\mp \pi^+ \pi^- \pi^0$.

an unseen neutral kaon (either K^0_1 or K^0_2), by use of the known geometrical efficiencies and $K^0_1 \to \pi^0\pi^0$ branching ratio.

The cross sections of table 5 show no significant evidence for any narrow direct channel resonances.

In figs. 2 and 3 some final state cross sections are plotted versus beam momentum, together with results‡ from other experiments [4–9].

5. $\bar{p}p \to K^0\bar{K}^0$

Cross sections, averaged over 1.76–1.94 GeV/c beam momentum, for $\bar{p}p \to K^0_1\bar{K}^0_1$ and $\bar{p}p \to K^0_1 K^0_2$ of 1 ± 1 μb and 5 ± 2 μb respectively, derived from 1,2–V event and 7,1–V events, give a total $\bar{p}p \to K^0\bar{K}^0$ cross section of 7 ± 2 μb. In comparison, the $\bar{p}p \to K^+K^-$ cross section at the same momenta is [10] 40 ± 4 μb. Thus the isospin zero and one amplitudes of $\bar{N}N \to K\bar{K}$ must be of the same order of magnitude, with their interference giving the large K^+K^- to $K^0\bar{K}^0$ ratio. In a simple exchange model, this result implies dominance of Λ exchange over Σ exchange. At 1.2 GeV/c, cross sections of [5] 6 ± 2 μb for $\bar{p}p \to K^0_1 K^0_1$ and 27 ± 5 μb for $\bar{p}p \to K^0_1 K^0_2$ give a $\bar{p}p \to K^0\bar{K}^0$ cross section of 39 ± 6μb, which can be compared to the $\bar{p}p \to K^+K^-$ cross section at 1.12 GeV/c of [11] 61 ± 4 μb.

The small number of events prevents any detailed study of $K^0\bar{K}^0$ angular distributions. However, the fact that 8 of the 10 $K^0_1(K^0)$ events (combining all incident momenta) have $|\cos\theta^*| < 0.5$, where θ^* is the c.m. production angle, suggests that the reaction is not strongly peripheral. In contrast, the $\bar{p}p \to K^+K^-$ reaction shows a clear forward peak at these momenta [10].

‡ The cross sections at 700 MeV/c are taken from the review of Montanet (ref. [4]).

6. $\bar{p}p \to K_1^0 K^{\pm}\pi^{\mp}$

A total of 228 events was assigned to these reactions, including 7 that were ambiguous between $K_1^0 K^+\pi^-$ and $K_1^0 K^-\pi^+$. In all effective mass plots, the events were weighted by the K_1^0 decay probability, and each ambiguous event was given an additional weight of 0.5 for each reaction. The effect of using unweighted events instead, or of choosing the best χ^2 of the ambiguous events is minute.

The effective mass plots, displayed in fig. 4 for all incident momenta combined, showed considerable $K^{*\pm}$ production but very little K^{*0}. A maximum likelihood fit to the Dalitz plot, assuming contributions from two incoherent K* Breit-Wigners and phase space (relativistic Breit-Wigners with the same mass and same constant width were used) gave a K* mass of 887 ± 5 MeV, K* width of 42 ± 8 MeV, and fractions of charged and neutral K* of 30 ± 5% and 3 ± 3% respectively, for all incident momenta combined (the errors quoted on the fractions were simply derived from the statistical errors on the number of events in the K* mass bands). For the four central momenta (1.76–1.94 GeV/c), the fractions found were 29 ± 6% and 1 ± 3%. Appeciable deviations from these average values were found at 1.94 and 2.20 GeV/c, where the charged K* fraction was ~ 12%, and at 1.62 GeV/c, where the neutral K* fraction was 12%. Thus there may be a sharp drop in the $K^{*\pm}K^{\mp}$ cross section at 1.91 GeV/c, and in the $K^{*0}K^0$ cross section at ~ 1.70 GeV/c, but better statistics are needed to confirm this.

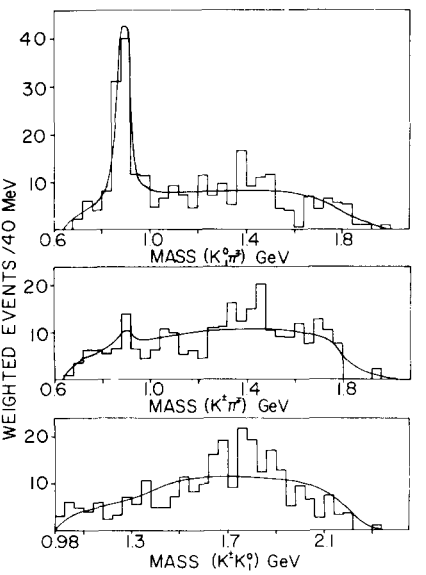

Fig. 4. Effective mass distributions for $K_1^0 K^{\pm}\pi^{\mp}$ events (all incident momenta). The curves are projections of the maximum likelihood fit.

The solid lines in fig. 4 are the projections of the maximum likelihood fit. There is no significant evidence for K*(1400) or any $K\bar{K}$ resonances.

The c.m. production angle for the $K^{\pm}$, with respect to the incident particle of like charge, is shown in fig. 5(a) and (b) for two selections on the $K_1^0\pi^{\mp}$ mass, (a) 840–940 MeV and (b) < 840 MeV plus 940–1240 MeV. There appears to be a forward peak in the $K^{*\pm}K^{\mp}$ reaction. The cosine of the decay angle θ (the Jackson angle, the angle between the $\bar{p}$ and π^- in the $K_1^0\pi^-$ rest frame or the p and the π^+ in the $K_1^0\pi^+$ rest frame) is shown in fig. 5(c) and (d) for the same two $K_1^0\pi^{\mp}$ mass selections. A non-isotropy appears in the K* mass band. The azimuthal angle distribution in the Jackson frame is flat for all $K_1^0\pi^{\mp}$ masses.

There is a very little K^{*0} signal in the K_1^0M or $K_1^0K\pi^0$ events, in agreement with the small $K_1^0K^{*0}$ signal in this reaction. In a simple exchange model, the large $K^{*\pm}K^{\mp}$ to $K^{*0}K^0$ ratio implies dominance of Λ exchange over Σ exchange, the same result as was found in the $\bar{K}K$ final state.

In the experiment at [5] 1.2 GeV/c, considerable amounts of $K^{*\pm}$ and K^{*0} were found in $K_1^0K^{\pm}\pi^{\mp}$ events, as well as possible $A_2 \to K\bar{K}$ and K*(1400). In a fit to the data without K*(1400), for which the evidence was not very strong, the resonance fractions found at 1.2 GeV/c were 28 ± 3% $K^{*\pm}$, 14 ± 3% K^{*0}, 7.5 ± 3% A_2. Thus, for a beam momentum change from 1.2 to 1.76–1.94 GeV/c, the $K_1^0K^{\pm}\pi^{\mp}$ cross section drops from 252 ± 15 μb to 102 ± 9 μb, the charged K* fraction remains constant, and the neutral K* fraction drops to nearly zero. The present 1.62 GeV/c data suggest that most of the cross section and K^{*0} decrease occurs between 1.62 and 1.76 GeV/c. In the related $K_1^0K_1^0\pi^0$ reaction, the cross section drops from 59 ± 7 μb at 1.2 GeV/c to 18 ± 5 μb at 1.76–1.95 GeV/c.

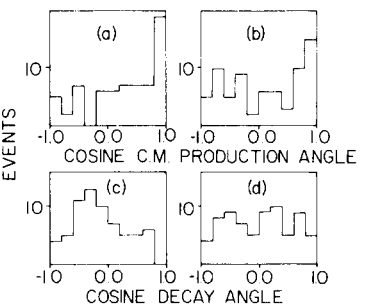

Fig. 5. Angular distributions for $K_1^0K^{\pm}\pi^{\mp}$ events. (a) $K^{\pm}$ c.m. production angle ($K^+\cdot p$ or $K^-\cdot\bar{p}$) for $K_1^0\pi^{\mp}$ mass 840–940 MeV; (b) as (a), but for $K_1^0\pi^{\mp}$ mass < 840 or 940–1240 MeV; (c) the decay angle of the $K_1^0\pi^{\mp}$ system ($\pi^-\cdot\bar{p}$ or $\pi^+\cdot p$ in $K_1^0\pi^{\mp}$ rest frame) for $K_1^0\pi^{\mp}$ mass 840–940 MeV; (d) as (c) but $K_1^0\pi^{\mp}$ mass < 840 or 940–1240 MeV.

7. $\bar{p}p \to K^{\pm}K_1^0\pi^{\mp}\pi^0$

A total of 599 events was assigned unambiguously to these two reactions, 325 $K^+K_1^0\pi^-\pi^0$ and 274 $K^-K_1^0\pi^+\pi^0$. In addition, 14 events were ambiguous between these two reactions and 83 events were ambiguous with $\bar{p}p \to K_1^0\pi^+\pi^-(K^0)$. In the maximum likelihood fits described below, the different possible fits of an ambiguous event were assumed to be equally probable, and so weights of 0.5 or 0.33 were given to each ambiguous $K^{\pm}K_1^0\pi^{\mp}\pi^0$ fit. If instead the fit with the lowest χ^2 was taken, the resulting fractional changes in the resonance fractions were less than 5%. All events were given a weight according to the probability that the K_1^0 decay in our fiducial volume, but the effect of this weight was very small (average weight was 1.17).

Effective mass plots showed considerable K* and ρ production, and no clear evidence of any other two– or three-body resonances. Hence a maximum likelihood fit was performed, assuming an incoherent sum of four $K^*K\pi$ channels, two K^*K^* channels, ρKK and simple $KK\pi\pi$ phase space. The matrix element for each resonance channel was written as a Breit-Wigner $(1/T \sim (m^2 - m_0^2)^2 + m_0^2\Gamma^2)$, or a product of two Breit-Wigners, with a constant width for the K* and a mass dependent width $(\Gamma = \Gamma_0\ (m_0/m)(q/q_0)^3$, where q is the breakup momentum of the $\pi^+\pi^-$ system with mass m) for the ρ. The K* and ρ masses (m_0) and widths (Γ_0) were set at 892, 50, 745, 145 MeV respectively, as suggested by some preliminary fits. (A fit to the mass interval 750–1000 MeV of the $K\pi$ mass plot for all constrained four-body reactions combined, with a Breit-Wigner and a constant background, gave a satisfactory fit with K* mass of 891 MeV and width of 45 MeV).

Table 7
Results of fit to $\bar{p}p \to K^{\pm}K_1^0\pi^{\mp}\pi^0$.

Channel	Percentages			
	All momenta		1.76–1.94 (GeV/c)	
$K^{*0}K_1^0\pi^0$	9 ± 2	10 ± 2	9 ± 2	11 ± 3
$K^{*0}K^{\pm}\pi^{\mp}$	7 ± 2	8 ± 2	8 ± 2	10 ± 3
$K^{*\pm}K_1^0\pi^{\mp}$	9 ± 2	14 ± 2	12 ± 2	17 ± 3
$K^{*\pm}K^{\mp}\pi^0$	17 ± 2	23 ± 3	17 ± 2	24 ± 3
$K^{*0}K^{*0}$	2 ± 1	0 a)	3 ± 1	0 a)
$K^{*+}K^{*-}$	8 ± 2	0 a)	8 ± 2	0 a)
$K^{\pm}K_1^0\rho^{\mp}$	25 ± 3	24 ± 4	26 ± 4	25 ± 5
$K^{\pm}K_1^0\pi^{\mp}\pi^0$	23	21	17	13
Log L	146	132	111	100

a) fixed at 0.

The fractions of each channel given by the maximum likelihood fit are listed in table 7, for all momenta combined and for the four central momenta combined, both with and without double-K* production. The quoted errors correspond to changes of 0.5 in the logarithm of the likelihood (as given by the program [12] MIGRAD). Fits at each momentum separately showed no appreciable deviations from the values of table 7 for the various fractions.

The presence of double-K* events was confirmed by studying a scatter plot of opposite $(K\pi)^{\pm}$ mass combinations. That area of the plot with both masses in the range 740–1040 MeV was subdivided into nine equal squares and the quantities A, B, C, were defined as follows: A as the number of events in the central square, C as the sum of the events in the four corner squares, and B as the sum of the events in the remaining four squares. Studies of phase space like $KK\pi\pi$, $K^*K\pi$, and K^*K^* events showed that the number of K^*K^* events at our momenta was given by $N =$

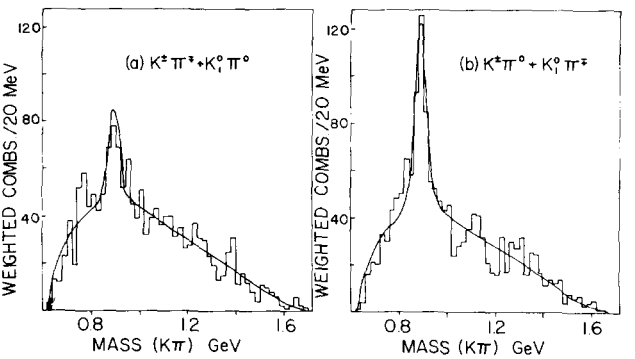

Fig. 6. $K\pi$ effective mass distributions for $K^0_1K^{\pm}\pi^{\mp}\pi^0$ events (all incident momenta). The curves are projections of the maximum likelihood fit.

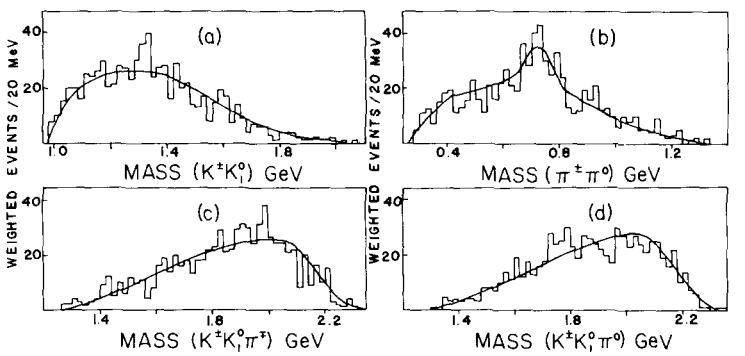

Fig. 7. KK, $\pi\pi$, and $KK\pi$ effective mass distributions for $K^0_1K^{\pm}\pi^{\mp}\pi^0$ events (all incident momenta). The curves are projections of the maximum likelihood fit.

Table 8
Comparison of $\bar{p}p \to K^{\pm}K^{0}_{1}\pi^{\mp}\pi^{0}$ at different incident momenta (resonance fractions in percentages).

Ref.	[13]	[5]	this expt.	[7]	[8]	[9]
Momentum (GeV/c)	0.7	1.2	1.76–1.94	2.7	3.0	3.7
Cross section (μb)	720 ± 35	590 ± 25	314 ± 17	175^{+40}_{-20}	275 ± 30	74^{+48}_{-36}
K^* a)	86 ± 4 b)	56 ± 4 c)	68 ± 4	40 ± 15	15 ± 10	45 ± 15
$K^{*+}K^{*-}$	18 ± 1	0 c)	8 ± 2	ns	ns	ns
$K^{*0}K^{*0}$	6 ± 1	0 c)	3 ± 1	ns	ns	ns
$KK\rho$ (inc. $A_2\rho$)	24 ± 2	20 ± 4	26 ± 4	7 ± 7	10 ± 10	8 ± 8
$A_2\pi\pi$ (inc. $A_2\rho$)	11 ± 1	5 ± 2	4 ± 2	ns	ns	ns

a) K^* means $K^*K\pi + 2K^*K^*$.
b) includes contributions from E, f', F_1 decays.
c) K^*K^* fractions were set to zero at 1.2 GeV/c.
ns) means not seen.

2.3 (A – 1.05 $B/2$ + 1.05 $C/4$). Applied to our data, this gave $K^{*+}K^{*-}$ fractions of 7.0 ± 3.0% and 7.2 ± 3.6% respectively for all momenta combined and for the four central momenta, in agreement with the maximum likelihood fit.

The mass distributions implied by the maximum likelihood fit are in reasonable agreement with the experimental mass distributions (fig. 6, 7). An excess of events at 1280–1340 MeV in the $K^{\pm}K^{0}_{1}$ mass spectrum may be attributed to the $A^{\pm}_{2}$, and suggests that 4.0 ± 1.5% of the events proceed via the channel $A^{\pm}_{2}\pi^{\pm}\pi^{0}$. There is no significant evidence for any other resonances; in particular there is less than 1% $D \rightarrow K^{\pm}K^{0}_{1}\pi^{\mp}$ and no strong threshold $\bar{K}K$ enhancement.

In table 8 results on this reaction in different experiments [5, 7–9, 13] are compared. Some caution is necessary here because of the differing methods used to obtain the resonance fractions. In addition, at the three higher momenta there are increasing numbers of ambiguous events, and the resonance fractions were determined from study of only the unambiguous events.

Each resonance fraction at 2.7, 3.0, and 3.7 GeV/c was determined by fitting to the appropriate mass spectrum a curve consisting of phase space and a Breit-Wigner (multiplied by phase space at 2.7 GeV/c), with reflections of other resonances taken into account at 2.7 and 3.7 GeV/c. At 1.2 GeV/c a maximum likelihood fit similar to ours was made, with double-K* production set to zero. At 0.7 GeV/c a maximum likelihood fit included D, E, f', F_1 resonances and a $\bar{K}K$ threshold enhancement (the latter was also included at 1.2 GeV/c).

The 1.2 GeV/c fit gave 19 ± 3% K^{*0} and 37 ± 3% $K^{*\pm}$, which agree well with our fit when the K^*K^* fractions are set to zero (columns 2 or 4 of table 7). The 0.7 GeV/c fit gave a total single K* fraction (including E, f', F_1 decays) of 38 ± 3%, with a breakdown into the four $K^*K\pi$ channels in reasonable agreement with ours when we allow non-zero K^*K^*. This 38 ± 3% also agrees with the K* fraction at 3.7 GeV/c. Thus it appears that in the $K^{\pm}K^{0}_{1}\pi^{\mp}\pi^{0}$ final state, the fraction of single K* production remains relatively constant at ~ 40% in the momentum range 0.7–3.7 GeV/c (assuming that K^*K^* production is small above ~ 2 GeV/c).

The ρ fraction appears to be constant from 0.7 to 2.0 GeV/c, but the ρA_2 component of this falls from 10 ± 1% at 0.7 GeV/c to ~ 0% at ~ 2.0 GeV/c. The appreciable $K\bar{K}$ threshold enhancement seen at 0.7 and 1.2 GeV/c does not appear at our momenta, and the significant $E^{0}\pi^{0}$ channel (5 ± 1%) seen at 0.7 GeV/c and not at 1.2 GeV/c is again not seen at our momenta, although an excess of 9 ± 5 events at 1380–1460 MeV in fig. 7(c) is compatible with 1.2 ± 0.7% $E^{0}\pi^{0}$.

8. $\bar{p}p \rightarrow K^{0}_{1}K^{0}_{1}\pi^{+}\pi^{-}$, $K^{0}_{1}K^{0}_{2}\pi^{+}\pi^{-}$

A total of 177 2–V events was assigned to the final state $K^{0}_{1}K^{0}_{1}\pi^{+}\pi^{-}$, with no ambiguities. 440 1–V events were assigned unambiguously to the final state $K^{0}_{1}(K^{0})\pi^{+}\pi^{-}$, where ($K^0$) denotes a missing neutral kaon, either a K^{0}_{2} or a K^{0}_{1} which decayed outside the bubble chamber or into $\pi^{0}\pi^{0}$, while 83 events were ambiguous

Table 9
Results of fits to $\bar{p}p \to K_1^0 K_1^0 \pi^+ \pi^-$ and $K_1^0(K^0)\pi^+\pi^-$.

Final state	Channel	Percentages			
		All momenta		1.76–1.94 GeV/c	
$K_1^0 K_1^0 \pi^+ \pi^-$	$K^{*\pm}K^0\pi^\mp$	47 ± 10	72 ± 8	39 ± 12	69 ± 9
	$K^{*+}K^{*-}$	17 ± 5	0 [a]	20 ± 6	0 [a]
	$K^0K^0\rho$	15 ± 6	15 ± 6	16 ± 7	16 ± 7
	$K^0K^0\pi^+\pi^-$	21	13	25	15
	Log L	45	37	34	26
$K_1^0(K^0)\pi$	$K^{*\pm}K^0\pi^\mp$	34 ± 6	63 ± 5	31 ± 8	60 ± 6
	$K^{*+}K^{*-}$	19 ± 3	0 [a]	18 ± 4	0 [a]
	$K^0K^0\rho$	13 ± 4	12 ± 4	15 ± 5	14 ± 5
	$K^0K^0\pi^+\pi^-$	34	25	36	26
	Log L	111	84	67	50
$K_1^0 K_2^0 \pi^+ \pi^-$	$K^{*\pm}K^0\pi^\mp$	28 ± 10	59 ± 8	27 ± 14	55 ± 11
	$K^{*+}K^{*-}$	20 ± 5	0 [a]	17 ± 7	0 [a]
	$K^0K^0\rho$	12 ± 7	11 ± 7	14 ± 9	13 ± 9
	$K^0K^0\pi^+\pi^-$	40	30	42	32

a) fixed at zero.

between $K_1^0(K^0)\pi^+\pi^-$ and one or both of $K_1^0 K^\pm \pi^\mp \pi^0$. The procedures described in the section on cross section determinations led to estimates that 47 ambiguous events belonged to the $K_1^0(K^0)\pi^+\pi^-$ final state, and that 326 of the 487 $K_1^0(K^0)\pi^+\pi^-$ events were $K_1^0 K_2^0 \pi^+ \pi^-$ events.

Maximum likelihood fits, similar to those for the $K_1^0 K^\pm \pi^\mp \pi^0$ final states, were made on the $K_1^0 K_1^0 \pi^+ \pi^-$ events and on the $K_1^0(K^0)\pi^+\pi^-$ events, with the same K* and ρ masses and widths. Ambiguous events were weighted by 0.5 or 0.33, but no geometrical weights were used (their effect on the fits is very small). The results are shown in table 9. The $K_1^0 K_2^0 \pi^+ \pi^-$ resonance fractions were calculated from the $K_1^0 K_1^0 \pi^+ \pi^-$ and $K_1^0(K^0)\pi^+\pi^-$ fractions, using the previously determined division of the $K_1^0(K^0)\pi^+\pi^-$ events. Again the presence of K*K* events was confirmed by a simple analysis of a $K\pi$ mass scatter plot, which gave K*K* fractions of 25 ± 8% and 18 ± 5% respectively for $K_1^0 K_1^0 \pi^+ \pi^-$ and $K_1(K_2)\pi^+\pi^-$ for all momenta combined.

The effective mass distributions implied by the fits give reasonable agreement with the experimental distributions, which are shown in fig. 8 for both final states

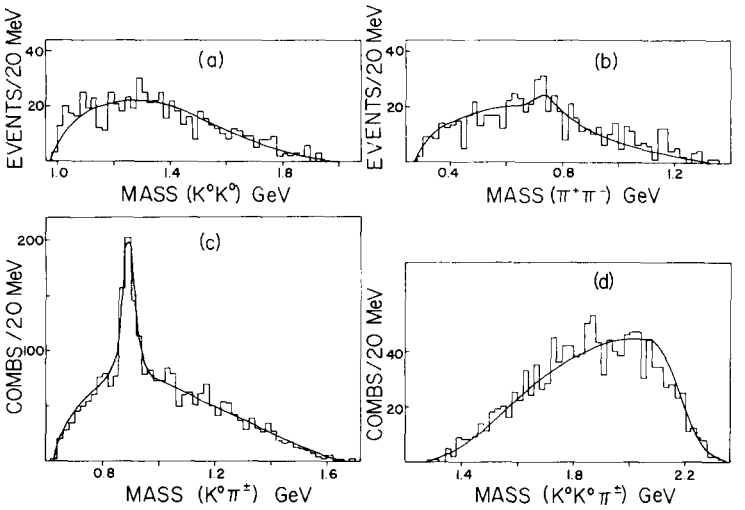

Fig. 8. Effective mass distributions for $K_1^0K_1^0\pi^+\pi^-$ and $K_1^0(K^0)\pi^+\pi^-$ events combined (all incident momenta). The curves are the sum of the projections of the maximum likelihood fits.

combined. The only appreciable difference between the two sets of mass plots was at low KK masses , an excess of 13 ± 4 events at 1015–1025 MeV in the $K_1^0(K^0)\pi^+\pi^-$ events indicates that 4 ± 1% of the $K_1^0K_2^0\pi^+\pi^-$ events proceed via the $\phi\pi^+\pi^-$ channel. No significant evidence for the production of any other resonances was found. Within the limited statistics there was no strong variation of the resonance fractions with momentum.

A maximum likelihood fit at [5] 1.2 GeV/c on $K_1^0K_1^0\pi^+\pi^-$ events assumed a matrix element squared for K* production of the form:

$$|T|^2 \sim |BW_a + BW_b + e^{i\phi}(BW_c + BW_d)|^2,$$

where $1/BW \sim m^2 - m_0^2 + im_0\Gamma$ and the subscripts (a,b) and (c,d) refer respectively to $K_1^0\pi^+$ and $K_1^0\pi^-$. combinations. The fit was not sensitive to the value of ϕ. In our fits we have used:

$$|T|^2 \sim |BW_a|^2 + |BW_b|^2 + |BW_c|^2 + |BW_d|^2.$$

The alternative expression above was tried on the $K_1^0K_1^0\pi^+\pi^-$ events, with ϕ set to zero, and resulted in a poorer fit and smaller K* fraction, viz. 56 ± 7% $K^*K^0\pi$, 13 ± 6% KKρ, Log L = 32, for all momenta combined, to be compared with the values in table 9.

Two internal consistency checks can be made between the $K^0\bar{K}^0\pi^\mp\pi^0$ final states. Simple isospin considerations lead to the predictions

Table 10
Comparison of $\bar{p}p \to K_1^0 K_1^0 \pi^+ \pi^-$ at different incident momenta (resonance fractions in percentages).

Ref.	[14]	[5]	this expt.	[7]	[8]	[9]
Momentum (GeV/c)	0.7	1.2	1.76–1.94	2.7	3.0	3.7
Cross section (μb)	238 ± 17	208 ± 20	136 ± 14	36 ± 16	70 ± 11	10 ± 3
$K^{*\pm} K_1^0 \pi^{\mp}$ a)	37 ± 5	b)	39 ± 12	c)	c)	38 ± 25
$K^{*+} K^{*-}$	22 ± 4	b)	20 ± 6	--	--	ns
$K_1^0 K_1^0 \rho$	12 ± 4	25 ± 8	16 ± 7	--	--	2 ± 2
$S^* \pi^+ \pi^-$	13 ± 3	12 ± 4	< 5 d)	--	--	--
$A_2 \pi^+ \pi^- + f \pi^+ \pi^-$	15 ± 5	20 ± 7	< 8 d)	--	--	--

a) includes K^*K^* (if any) only at 3.7 GeV/c, includes $F_1 \to K^*K$ at 0.7 GeV/c.
b) fit at 1.2 GeV/c uses different K^* matrix element.
c) no results given for this reaction.
d) two standard deviation upper limit.

Table 11
Comparison of $\bar{p}p \to K_1^0 K_2^0 \pi^+ \pi^-$ at different incident momenta (resonance fractions in percentages).

Ref.	14	15	this expt.
Momentum (GeV/c)	0.7	1.1–1.2	1.76–1.94
Cross section (μb)	280 ± 23		153 ± 17
$K^{*\pm}K^0\pi^\mp$ a)	57 ± 5	42 ± 5	27 ± 14
$K^{*+}K^{*-}$	23 ± 3	27 ± 3	17 ± 7
$K^0K^0\rho$	0 ± 2	2 ± 2	14 ± 9
$\phi\pi^+\pi^-$	5 ± 1	7 ± 1	4 ± 1
$F_1^\pm\pi^\mp$	14 ± 3	3 ± 1	ns

a) excludes K^*K^*, includes $F_1 \to K^*K$.

$$\sigma(K^{*+}K^{*-} \to K^0\bar{K}^0\pi^+\pi^-) - \sigma(K^{*+}K^{*-} \to K^\pm K^0\pi^\mp\pi^0) = 0 \ ,$$

$$\sigma(K^{*\pm}K^0\pi^\mp \to K^0\bar{K}^0\pi^+\pi^-) - 2\sigma(K^{*\pm}K^0\pi^\mp \to K^\pm K^0\pi^\mp\pi^0) = 0 \ .$$

Our fits and cross sections give for the left hand side of the first equation 67 ± 16 – 52 ± 8 = 24 ± 18 μb and for the second equation 164 ± 29 – 116 ± 16 = 48 ± 33 μb. In both cases, there is about a 1.5 standard deviation disagreement with the prediction. This may indicate that the matrix elements used in the fitting are inadequate, but clearly a higher statistics experiment is needed to confirm the disagreement. We note that at 0.7 GeV/c the published fits [14] and cross sections [4] give 169 ± 40 – 260 ± 20 = – 91 ± 45 μb and 336 ± 32 – 316 ± 32 = 20 ± 45 μb respectively.

Comparison of the $K_1^0K_1^0\pi^+\pi^-$ final state in different experiments [5, 7–9, 14] is made in table 10. As in the $K^\pm K_1^0\pi^\mp\pi^0$ case, there appears to be some disagreement between the 2.7 and 3.0 GeV/c cross sections, unless there is some unusual behavior near these momenta. The single K* fraction may again be approximately constant with momentum, but, contrary to the $K^\pm K_1^0\pi^\mp\pi^0$ case, the $K^{*+}K^{*-}$ fraction does not appear to fall between 0.7 and ~ 1.8 GeV/c.

Results on the $K_1^0K_2^0\pi^+\pi^-$ final state have been reported [14, 15] at 0.7 and 1.1–1.2 GeV/c, and are compared with our results in table 11.

9. $\bar{p}p \to K^\pm K_1^0\pi^\mp\pi^+\pi^-$

The number of events assigned to this reaction was 347, with no unresolved ambiguities. A study of this reaction, with emphasis on the energy dependence of the total cross section and the K* production cross section, within our energy range, has been reported [1]. Maximum likelihood fits to the events have now been performed, to determine fractions of K*, ρ, and associated production.

Table 12
Results of fits to $\bar{p}p \to K^{\pm}K_1^0\pi^{\pm}\pi^+\pi^-$.

Channel	Percentages			
	All momenta		1.76–1.94 GeV/c	
$K^{*0}K_1^0\pi^+\pi^-$	2 ± 2	26 ± 5	5 ± 7	26 ± 6
$K^{*\pm}K^{\mp}\pi^+\pi^-$	0 ± 2	31 ± 5	0 ± 2	30 ± 6
$K^{\pm}K_1^0\pi^{\mp}\rho$	24 ± 8	43 ± 6	29 ± 8	45 ± 7
$K^{*0}K^{*\pm}\pi^{\mp}$	17 ± 4	0 a)	18 ± 6	0 a)
$K^{*0}K_1^0\rho$	22 ± 6	0 a)	20 ± 8	0 a)
$K^{*\pm}K^{\mp}\rho$	31 ± 5	0 a)	28 ± 8	0 a)
$K^{\pm}K^0\pi^{\mp}\pi^+\pi^-$	4	0	0	0
Log L	151	116	107	84

a) fixed at zero

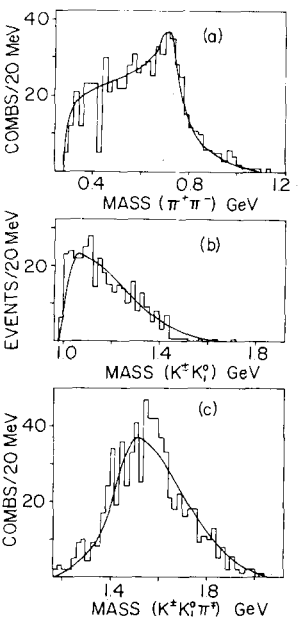

Fig. 9. Effective mass distributions for $K_1^0K^{\pm}\pi^{\mp}\pi^+\pi^-$ events (all incident momenta). The curves are projections of the maximum likelihood fit.

Table 13
Comparison of $\bar{p}p \to K^{\pm}K_1^0\pi^{\mp}\pi^+\pi^-$ at different incident momenta (resonance fractions in percentages).

Ref.	[6]	This expt.	[7]	[8]	[9]
Momentum (GeV/c)	1.2	1.76–1.94	2.7	3.0	3.7
Cross section (μb)	105 ± 10	189 ± 14	151 ± 26	177 ± 26	97^{+41}_{-14}
K^* a) (inc. $K^*\rho$)	67 ± 4 b)	89 ± 12	75 ± 15	60 ± 15	75 ± 15
ρ (inc. $K^*\rho$)	30 ± 5	77 ± 10	40 ± 10	35 ± 10	25 ± 10
K^*K^*	0 b)	18 ± 6	ns	20 ± 5	ns
$K^*\rho$	0 b)	48 ± 11	15 ± 10	ns	ns

a K^* means $K^*K\pi\pi + 2K^*K^*\pi$.
b K^*K^* fractions were set to zero at 1.2 GeV/c.
ns means not seen.

The maximum likelihood fits assumed K^{*0}, $K^{*\pm}$, and ρ resonances were present, singly and in pairs, and the matrix elements used were the same as in the four-body fits described above. The K^* and ρ mass and width were again set at 892, 50, 745, 145 MeV respectively. Changes of ± 20 MeV in the ρ width or ± 10 MeV in the ρ mass led to slightly smaller values of the likelihood function and to the same resonance fraction, within the stated errors. Unweighted events were used in the fits; introduction of a geometrical K_1^0 decay weight gave negligible changes.

Results of the fits are given in table 12. Fits at individual momenta showed no strong deviations from these combined values; There is clearly much associated production of resonances: the three-body channels account for ~ 70% of the reaction. Table 12 gives a total K^* fraction per event of 0.89 (all momenta combined), which agrees well with the value of 0.93 ± 0.10 from ref. [1], where these fractions were obtained directly from the $K\pi$ mass spectra.

The experimental mass distributions are in reasonable agreement with the distributions implied by the fit (fig. 9). An excess of events does appear at the low mass end of the $\bar{K}K$ mass spectrum; the excess over the curve below 1040 MeV is 20 ± 7 events, corresponding to 6 ± 2% of the reaction.

In table 13 our results are compared with experiments at other momenta [6–9]. The resonance fractions at 1.2 GeV/c come from a simultaneous fit to all two- and three-body mass spectra, without allowance for associated production (except $D\rho$); those at the higher momenta come from simple fits to the mass spectra using only unambiguous events. It is difficult to draw any conclusion from table 13, outside of the fact that the total K^* production appears to remain relatively constant. Our data are compatible with 2 ± 2% $D\pi\pi$ and 4 ± 3% $E\pi\pi$, whereas at [6] 1.2 GeV/c the $D\pi\pi$ channel accounted for 6 ± 2% of the reaction and the $E\pi\pi$ channel accounted for ~ 60% of the reaction at 0.7 GeV/c and 9 ± 3% (estimated from the published fig. 8) at 3.0–4.0 GeV/c.

10. $\bar{p}p \to K_1^0 K_1^0 \pi^+ \pi^- \pi^0$

A total of 207 events, all unambiguous, were assigned to this reaction.

In ref. [1] we reported on this reaction, and in particular on the incident moment variation, within our momentum range, of the K* and ω production cross sections. No maximum likelihood fits have been made, because of the relatively low statistics and large number of different channels. Instead, fractions of $K^{*\pm}$, K^{*0}, and ω for the four central momenta were taken from ref. [1], and then various mass distributions were generated assuming the appropriate numbers of $KK\omega$, $K^*K\pi\pi$, and $KK\pi\pi\pi$ events. The deviations of the experimental mass distributions from the generated ones were then used to estimate the amounts of charged and neutral ρ present and to look for any other resonances (see fig. 10).

Our results, and those obtained in other experiments [6–9], are shown in table 14. The resonance fractions in the other experiments were determined in exactly the same way as for the $K^{\pm}K_1^0\pi^{\mp}\pi^+\pi^-$ final state. The table shows a decreasing ω fraction, an apparently increasing ρ fraction, and a relatively constant K* fraction, although the K* fraction at 1.76–1.96 GeV/c is slighly higher than other momenta. The total cross section value at 3.0 GeV/c appears to be anomalously large.

The breakdown into charged and neutral meson production in our data gives 57 ± 14% and 19 ± 9% respectively for the K*, and 10 ± 5% and 0 ± 3% for ρ. An excess of events at low KK mass was also observed in our data, the excess below 1040 MeV amounting to 8 ± 3% of the events. We see less than 1% D meson production.

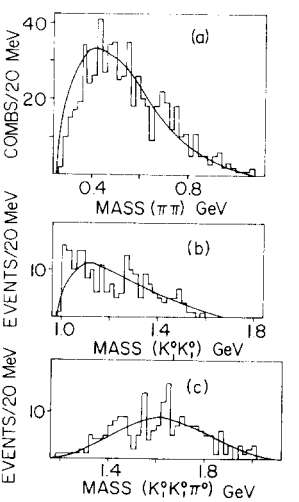

Fig. 10. Effective mass distributions for $K_1^0 K_1^0 \pi^+ \pi^- \pi^0$ events (all incident momenta). The curves assume contributions from $KK\omega$, $K^*K\pi\pi$, and $KK\pi\pi\pi$ events, with ω and K* fractions taken from ref. [1].

Table 14
Comparison of $\bar{p}p \to K_1^0 K_1^0 \pi^+ \pi^- \pi^0$ at different incident momenta (resonance fractions in percentages).

Ref.	[6]	this expt.	[7]	[8]	[9]
Momentum (GeV/c)	1.2	1.76–1.94	2.7	3.0	3.7
Cross section	186 ± 17	151 ± 15	69 ± 21	139 ± 18	34^{+5}_{-11}
K^{*} a) (inc. $K^{*}\rho$)	40 ± 5	76 ± 16	40 ± 10	50 ± 20	30 ± 15
ω	43 ± 3	24 ± 4	6 ± 6	ns	5 ± 5
ρ (inc. $K^{*}\rho$)	16 ± 5	10 ± 6	10 ± 5	40 ± 20	40 ± 15

a) K^{*} means $K^{*}K\pi\pi + 2K^{*}K^{*}\pi$.
ns) means not seen.

11. $\bar{p}p \to K^{\pm}K_1^0\pi^{\mp}$(M)

There were 332 unambiguous events of this reaction, where M implies more than one missing neutral particle. In addition, 120 events were ambiguous between one or both of these final states and $K_1^0\pi^+\pi^-$(M). This reaction is of interest because of the observation [15] at 1.1–1.2 GeV/c of the D and F_1 mesons in the $KK\pi$ mass spectrum. In our study of the reaction, only the 332 unambiguous events have been considered.

Reasonable agreement with the missing mass spectrum and the $K^{\pm}\pi^{\mp}$ and $K_1^0\pi^{\mp}$ mass spectra was obtained by assuming a mixture of 70% $K^{\pm}K_1^0\pi^{\mp}\pi^0\pi^0$ events and 30% $K^{\pm}K_1^0\pi^{\mp}\pi^0\pi^0\pi^0$ events, each with 11% $K^{*0} \to K^{\pm}\pi^{\mp}$ and 20% $K^{*\pm} \to K_1^0\pi^{\pm}$. The $K^{\pm}K_1^0$ and $K^{\pm}K_1^0\pi^{\mp}$ mass spectra of this model were then compared with the experimental ones (fig. 11).

The experimental $\bar{K}K$ spectrum shows an excess at low mass (< 1040 MeV) amounting to 6 ± 2% of the events, the same fraction as in the $K^{\pm}K_1^0\pi^{\mp}\pi^+\pi^-$ final state. The $K^{\pm}K_1^0\pi^{\mp}$ mass spectrum shows an excess of events in the D region (1260–1320 MeV) of 10 ± 5 events or 3 ± 1.5% and a narrow enhancement at 1400–1440 MeV of 15 ± 6 events (5 ± 2%), which could be due to the E meson, although the width of the latter is [13, 16] 60–80 MeV. In the F_1 region (1520–1560 MeV) we find a deficiency of 3 ± 5 events.

This same final state at 1.1–1.2 GeV/c showed 18 ± 5% D production [6], three times the percentage in the $K^{\pm}K_1^0\pi^{\mp}\pi^+\pi^-$ events at that momentum, and ~ 6 ± 1% F_1 production [15]. Most of this F_1 production was in the 2–body channel $F_1\eta$. Our missing mass spectrum indicates some η production, 20 ± 7 events above background, but the $K_1^0K^{\pm}\pi^{\mp}$ mass spectrum for those events with missing mass in the η region (520–580 MeV) shows no signal in the F_1 region, although there are 6 Dη events (see fig. 11(b)).

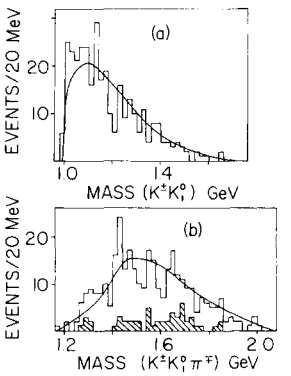

Fig. 11. Effective mass distributions for unambiguous $K^{0}_{1}K^{\pm}\pi^{\mp}M$ events (all incident momenta). The curves assume 70% $K^{0}_{1}K^{\pm}\pi^{\mp}\pi^{0}\pi^{0}$, 30% $K^{0}_{1}K^{\pm}\pi^{\mp}\pi^{0}\pi^{0}\pi^{0}$, each with 31% $K^{*} \rightarrow K\pi^{\mp}$ (see text). Shaded events in (b) have missing mass (M) in the range 520–580 MeV

12. $\bar{p}p \rightarrow K^{\pm}K^{0}_{1}\pi^{\mp}\pi^{+}\pi^{-}\pi^{0}$

A total of 195 events was unambiguously assigned to this reaction.

The $\pi^{+}\pi^{-}\pi^{0}$ mass spectrum shows that ω production is very strong. A fit to this spectrum, for all momenta combined, assuming contributions from six-body phase space and the $K^{\pm}K^{0}_{1}\pi^{\mp}\omega$ channel, showed that 59 ± 7% of the events proceed via ω production, or 56 ± 8% for the four central momenta. No maximum likelihood fits have been performed because of the large number of possible channels. Instead the mass spectra have been compared to the predictions of a mixture of 41% six-body phase space and 59% $K^{\pm}K^{0}_{1}\pi^{\mp}\omega$ (or 44% and 56% respectively for the four central

Table 15
Comparison of $\bar{p}p \rightarrow K^{\pm}K^{0}_{1}\pi^{\mp}\pi^{+}\pi^{-}\pi^{0}$ at different incident momenta (resonance fractions in percentages).

Ref.	[6]	this expt.	[7]	[8]	[9]
Momentum (GeV/c)	1.2	1.76–1.94	2.7	3.0	3.7
Cross section (μb)	46 ± 6	102 ± 9	182 ± 30	237 ± 20	201^{+47}_{-75}
ω (inc. Dω)	65 ± 9	56 ± 8	30 ± 10	15 ± 5	20 ± 10
D (inc. Dω)	47 ± 7	16 ± 5	ns	ns	ns
K^{*} [a] (inc. $K^{*}\rho$,$K^{*}\omega$)	35 ± 13	22 ± 8	50 ± 15	60 ± 10	50 ± 10
ρ (inc. $K^{*}\rho$)	—	7 ± 5	15 ± 15	50 ± 20	30 ± 10

a) K^{*} means $K^{*}K\pi\pi\pi + 2K^{*}K^{*}\pi\pi$.
ns) means not seen.

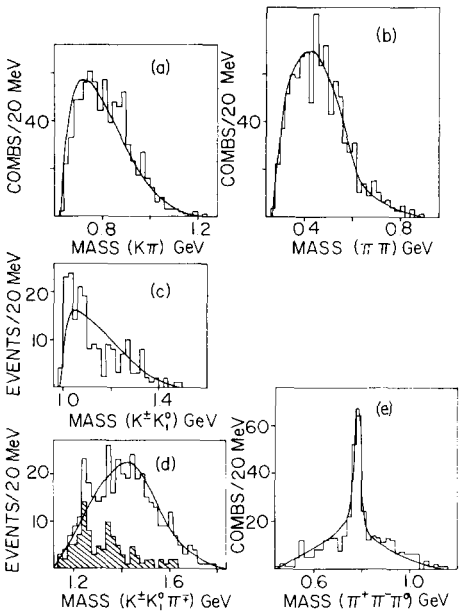

Fig. 12. Effective mass distributions for $K^0_1K^{\pm}\pi^{\mp}\pi^+\pi^-\pi^0$ events (all incident momenta). The curves assume 59% $K^0_1K^{\pm}\pi^{\mp}\omega$ and 41% 6–body phase space. The shaded events in (d) have $K^0_1K^{\pm}$ mass less than 1040 MeV.

momenta) (see fig. 12). There is marginal evidence for ρ production, some $K^* \to K\pi^{\pm}$ but no $K^* \to K\pi^0$, some $D \to K^{\pm}K^0_1\pi^{\mp}$, and a low mass KK enhancement most of which is associated with the D. Estimates of ω, ρ, K^*, and D percentages for the four central momenta are listed in table 15, together with results of other experiments [6–9] (where the methods used were the same as in the five-body final states).

Table 15 shows a roughly constant K^* fraction, but the ω and D fractions decrease with increasing momentum. At [6] 1.2 GeV/c all the D meson production was associated with the ω (apart from 1 ± 1% Dη). In our data the ratio of Dω to all D events is estimated to be 0.50 ± 0.20. A search for ωK^* associated production in our data showed that 70 ± 20% of the K^*s occur in $K^*K\omega$ events.

13. $\bar{p}p \to KKKK$

In the 2–V events, there was 1 $K^0_1K^0_1K^+K^-$ event. This event was at 2.20 GeV/c, and corresponds to a cross section (corrected for invisible decays) of 4 μb at 2.20 GeV/c.

Of the 1–V 2–prong events, 10 were unambiguous $K^0_1(K^0)K^+K^-$ events, and a

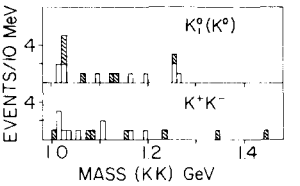

Fig. 13. $K^0_1(K^0)$ and K^+K^- effective mass distributions for $K^0_1(K^0)K^+K^-$ events. The shaded events are ambiguous with two-kaon final states.

further 7 were ambiguous between this final state and one or more two-kaon final states. The incident momentum distribution of these events was 0, 1, 6, 0, 2, 1 for the unambiguous events and 0, 1, 1, 1, 1, 3 for the ambiguous events (incident momenta in order lowest to highest, i.e. 1.62 to 2.20 GeV/c). If the number of real $K^0_1(K^0)K^+K^-$ events is taken to be 14 ± 4, and 1 ± 1 of these are $K^0_1K^0_1K^+K^-$ events, a momentum averaged cross section of 6.5 ± 2.5 μb results (or 8.0 ± 3.0 μb for 1.76–1.94 GeV/c), for $\bar{p}p \to K^0_1K^0_2K^+K^-$.

The K^+K^- and $K^0_1(K^0)$ mass spectra for these events (fig. 13) show evidence of ϕ production. Of the total of 17 events, 7 have $K^0_1(K^0)$ mass in the range 1014–1024 MeV, and 4 have K^+K^- mass in this range. Two events, both unambiguous, have both KK masses in this range, and lead to an estimate of 3 ± 1.5 μb for the $\bar{p}p \to \phi\phi$ cross section (all decay modes).

14. CONCLUSIONS

We have determined cross sections, and the percentage contributions of various resonance channels, for several final states that result from antiproton proton annihilations and that include a K^0_1 meson. Our results do not show any dependence on incident momentum that would suggest the presence of direct channel resonances. There may be a sharp drop in the $K^0K^\pm\pi^\mp$ cross section near 1.7 GeV/c.

Strong production of K^*, ρ and ω mesons is observed. These resonances appear in all final states where they are allowed by their decay properties. The ϕ meson also occurs in the two final states that contain its $K\bar{K}$ decay mode, but with small cross section.

Cross sections for various resonance and non-resonance channels, computed from our cross sections and fits for the 1.76–1.94 GeV/c incident momenta, are given in table 16. (The fits, and hence the cross sections, assume that the different channels are incoherent.) The non-resonance cross sections (e.g. $K^\pm K^0\pi^\mp\pi^0$) were calculated from the percentage of Lorentz-invariant phase space given by the maximum likelihood fits, minus the percentage of any resonances observed but not included in the fits (e.g. $A_2 \to K^\pm K^0$). The different channels in the table are all mutually exclusive.

Table 16
Channel cross sections at 1.76–1.94 GeV/c.

Channel [a]	Cross section (μb)	Channel [a]	Cross section (μb)
K^+K^-	40 ± 4	$K^{*\pm}(K\pi)^{\mp}$	381 ± 61
$K^0_1K^0_1$	1 ± 1	$K^{*0}(K\pi)^0$	236 ± 43
$K^0_1K^0_2$	5 ± 2	$(K\bar{K})^{\pm}\rho^{\mp}$	163 ± 25
$K^{*\pm}K^{\mp}$	89 ± 18	$K^0K^0\rho^0$	65 ± 24
$K^{*0}K^0$	3^{+9}_{-3}	$K^{*\pm}K^{*0}\pi^{\mp}$	153 ± 51
$K^{*+}K^{*-}$	146 ± 26	$(K^*K)^0\rho^0$	272 ± 64
$K^{*0}K^{*0}$	42 ± 14	$\phi\pi^+\pi^-$	17 ± 5
$D\omega(D\to K^{\pm}K^0\pi^{\mp})$	18 ± 9	$K^0_1K^0_1\omega$	40 ± 7
		$(K^*K)^0\omega$	52 ± 24
$K^{*\pm}(K^{\mp}\pi^+\pi^-)$	0^{+11}_{-0}	$K^{\pm}K^0\pi^{\mp}$	143 ± 14
$K^{*0}(K^0\pi^+\pi^-)$	28^{+40}_{-28}	$K^0_1K^0_1\pi^0$	18 ± 5
$(K^{\pm}K^0\pi^{\mp})\rho^0$	110 ± 30		
$(K^{\pm}K^0\pi^{\mp})\omega$	14 ± 10	$K^{\pm}K^0\pi^{\mp}\pi^+\pi^-$	0^{+38}_{-0}
$K^{\pm}K^0\pi^{\mp}\pi^0$	82 ± 25		
$K^0K^0\pi^+\pi^-$	126 ± 20		

a) K^0 means K^0_1 and K^0_2. K^*, ω, ϕ include all decay modes.

The table shows that (pseudo–) 3 body channels have generally larger cross sections than 2, 4 or 5 body channels, although it is difficult to make a strong statement here because some channels are not observable in this experiment and are not listed in the table. The large charged to neutral ratio seen in the K*K and K*K* channels, and also in the $K\bar{K}$ final state, suggests a simple hyperon exchange model in which isospin-zero exchange is dominant.

We have compared the resonance fraction in our final states with results from other experiments in the incident momentum range 0.7 to 3.7 GeV/c. The comparison is not completely straightforward because of the different methods used to determine the resonance fractions and the different resonance channels that are assumed to be present. However, it does appear that the fractions of K* and ρ are roughly constant over the 0.7 to 3.7 GeV/c momentum range, while the ω fraction decreases with increasing momentum. Of the three $K\bar{K}\pi$ resonances, the D, E, and F_1 mesons, seen at lower momenta, there is significant evidence in this experiment only for the D, and that only in the 6 body final state $K^0_1K^{\pm}\pi^{\mp}\pi^+\pi^-\pi^0$. The 5 and 6 body final states, but not the 3 and 5 body ones, show small but significant low mass $K\bar{K}$ enhancements.

We are indebted to Dr. F. Schweingruber, Dr. L. Voyvodic and the crew of the 30–inch bubble chamber at Argonne National Laboratory. We thank J. Davidson and A. Vandermolen for their assistance with the bubble density scan.

REFERENCES

[1] J.W. Chapman, R. Green, J. Lys, C.T. Murphy, H.M. Ring, and J.C. Vander Velde, Phys. Rev. D4 (1971) 1275.
[2] H.M. Ring, Ph.D. thesis, University of Michigan, 1970 (unpublished).
[3] T.M. Church, Ph.D. thesis, University of Michigan (in preparation).
[4] L. Montanet, Proc. of the Lund Conf. on elementary particles (1969) 191.
[5] J. Barlow, E. Lillestøl, L. Montanet, L. Tallone-Lombardi, C. d'Andlau, A. Astier, L. Dobrzynski, S. Wodjcicki, A.M. Adamson, J. Duboc, F. James, M. Goldberg, R.A. Donald, R. James, J.E.A. Lys, and T.Nisar, Nuovo Cimento 50A (1967) 701.
[6] C. d'Andlau, A. Astier, L. Dobrzynski, J. Siaud, J. Barlow, L. Montanet, L. Tallone-Lombardi, A.M. Adamson, J. Duboc, M. Goldberg, R.A. Donald, D.N. Edwards, and J.E.A. Lys, Nucl. Phys. B5 (1968) 693.
[7] L.S. Schroeder, W.J. Kernan, G.P. Fisher, A.J. Eide, J. von Krogh, L. Marshall Libby, and R. Sears, Phys. Rev. 188 (1969) 2081.
[8] B.R. French, J.B. Kinson, R. Rigopoulos, V. Simak, F. McDonald, G. Petmezas, and L. Riddiford, Nuovo Cimento 52A (1967) 438.
[9] C. Baltay, J. Lach, J. Sandweiss, H.D. Taft, N. Yeh, D.L. Stonehill, and R. Stump, Phys. Rev. 142 (1966) 932.
[10] J.W. Chapman, F. Hess, J. Lys, C.T. Murphy, and J.C. Vander Velde, Phys. Rev. Letters 21 (1968) 1718.
[11] H. Nicholson, B.C. Barish, J. Pine, A.V. Tollestrup, J.K. Yoh, C. Delorme, F. Lobkowicz, A.C. Melissinos, Y. Nagashima, A.S. Carroll, and R.H. Phillips, Phys. Rev. Letters 23 (1969) 603.
[12] F. James and M. Roos, "Minuit", Cern D506, 1969 (unpublished).
[13] B. Lorstad, C. d'Andlau, J. Cohen-Ganouna, M. Della-Negra, M. Aguilar-Benitez, J. Barlow L.D. Jacobs, P. Malecki, and L. Montanet, Nucl. Phys. B14 (1969) 63.
[14] M. Aguilar-Benitez, J. Barlow, L.D. Jacobs, P. Malecki, L. Montanet, C. d'Andlau, A. Astier, J. Cohen-Ganouna, M. Della-Negra, and B. Lorstad, Nucl. Phys. B14 (1969) 195.
[15] J. Duboc, M. Goldberg, B. Makowski, A.W. Touchard, R.A. Donald, D.N. Edwards, J. Galletly, and N. West, Phys. Letters 34B (1971) 343).
[16] P. Baillon, D. Edwards, B. Marechal, L. Montanet, M. Tomas, C. d'Andlau, A. Astier, J. Cohen-Ganouna, M. Della-Negra, S. Wojcicki, M. Baubillier, J. Duboc, F. James and F. Levy, Nuovo Cimento 50A (1967) 393.